

AMR Simulations of Pellet Injection

Ravi Samtaney

Computational Plasma Physics Group
Princeton Plasma Physics Laboratory
Princeton University

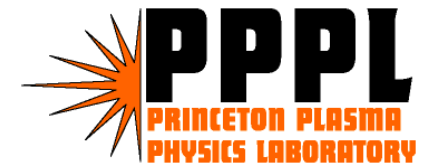


CEMM Meeting,
April 27, 2003
Corpus Christi, TX



Collaborators

- Phillip Colella, LBNL
- Steve Jardin, PPPL
- Terry Ligocki, LBNL
- Dan Martin, LBNL



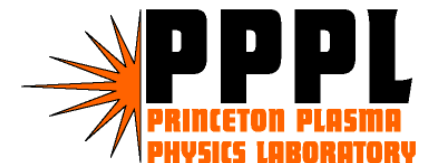
Outline

- Semi-implicit MHD code – Progress
- 3D AMR MHD code
- Pellet Injection - Progress
- Conclusion and future work



3D AMR MHD Code - Status

- Hyperbolic fluxes computed using an unsplit upwind method
- Implicit treatment of parabolic terms
- $\mathbf{r} \cdot \mathbf{B} = 0$ by projection
- Inclusion of nonlinear coefficients in the elliptic solvers is under progress
 - *Reconnection (with Breslau's nonlinear \mathbf{h}) will be the test case*



Single-fluid resistive MHD Equations

- Equations in conservation form

$$\frac{\partial U}{\partial t} + \frac{\partial F_j(U)}{\partial x_j} = \frac{\partial \tilde{F}_j(U)}{\partial x_j}$$

Parabolic

Hyperbolic

$$U = \{\rho, \rho u_i, B_i, e\}^T$$

$$F_j(U) = \left\{ \begin{array}{l} \rho u_j \\ \rho u_i u_j + p \delta_{ij} + \frac{1}{2} B_k B_k \delta_{ij} - B_i B_j \\ u_j B_i - B_j u_i \\ (e + p + \frac{1}{2} B_k B_k) u_j - B_i u_i B_j \end{array} \right\}$$

$$\tilde{F}_j(U) = \left\{ \begin{array}{l} 0 \\ Re^{-1} \tau_{ij} \\ S^{-1} \eta \left(\frac{\partial B_i}{\partial x_j} + \frac{\partial B_j}{\partial x_i} \right) \\ S^{-1} \eta \left(\frac{1}{2} \frac{\partial B_i B_i}{\partial x_j} - B_i \frac{\partial B_j}{\partial x_i} \right) + Re^{-1} \tau_{ij} u_i + Pe^{-1} \kappa \frac{\partial T}{\partial x_j} \end{array} \right\}$$

Reynolds no.

Lundquist no.

Peclet no.

$$\tau_{ij} = \rho \nu \left(\frac{\partial u_i}{\partial x_j} + \frac{\partial u_j}{\partial x_i} - \frac{2}{3} \delta_{ij} \frac{\partial u_k}{\partial x_k} \right)$$

$$e = \frac{p}{\gamma - 1} + \frac{1}{2} \rho u_i u_i + \frac{1}{2} B_i B_i$$



Numerical Method

- MHD Equations written in symmetrizable near-conservative form (Godunov, Numerical Methods for Mechanics of Continuum Media, 1, 1972, Powell et al., J. Comput. Phys., vol 154, 1999).

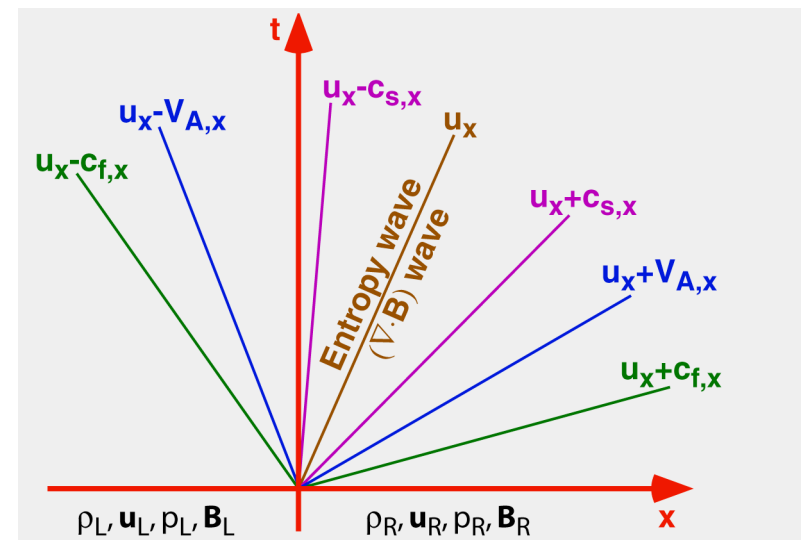
– Deviation from total conservative form is of the order of $\tilde{N} \times \mathbf{B}$ truncation errors

$$\frac{\partial}{\partial t} \begin{pmatrix} r \\ \mathbf{ru} \\ \frac{1}{2} r u^2 + \frac{1}{g-1} p + \frac{1}{2m_0} B^2 \\ \mathbf{B} \end{pmatrix} + \left\{ \nabla \cdot \begin{pmatrix} \mathbf{ru} \\ r\mathbf{uu} + \left(p + \frac{1}{2m_0} B^2\right) \mathbf{I} - \frac{1}{m_0} \mathbf{BB} \\ \left[\frac{1}{2} r u^2 + \frac{p}{g-1} + \frac{1}{2m_0} B^2\right] \mathbf{u} - \frac{1}{m_0} (\mathbf{u} \cdot \mathbf{B}) \mathbf{B} \\ \mathbf{uB} - \mathbf{Bu} \end{pmatrix} \right\}^T = -(\nabla \cdot \mathbf{B}) \begin{pmatrix} 0 \\ \frac{1}{m_0} \mathbf{B} \\ \frac{1}{m_0} (\mathbf{u} \cdot \mathbf{B}) \\ \mathbf{u} \end{pmatrix}$$

- The symmetrizable MHD equations lead to the 8-wave method.
 - The fluid velocity advects both the entropy and $\text{div}(\mathbf{B})$
- Finite volume approach. Hyperbolic fluxes determined using the unsplit upwinding method (Colella, J. Comput. Phys., Vol 87, 1990)
 - Predictor-corrector.
 - Fluxes obtained by solving Riemann problem
 - Good phase error properties due to corner coupling terms

$$U_i^{n+1} = U_i^n - \frac{\Delta t}{h} \sum_{d=0}^{D-1} (F_{i+\frac{1}{2}e^d}^{n+\frac{1}{2}} - F_{i-\frac{1}{2}e^d}^{n+\frac{1}{2}})$$

$$F_{i+\frac{1}{2}e^d}^{n+\frac{1}{2}} = R(W_{i,+,d}^{n+\frac{1}{2}}, W_{i+e^d,-,d}^{n+\frac{1}{2}}, d)$$



$\mathbf{r} \cdot \mathbf{B} = 0$ by Projection

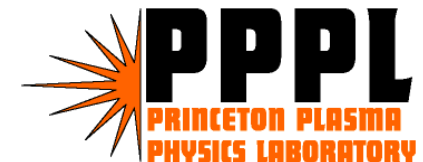
- Compute the estimates to the fluxes $F^{n+1/2}_{i+1/2,j}$ using the unsplit formulation
- Use face-centered values of B to compute $\mathbf{r} \cdot \mathbf{B}$.
Solve the Poisson equation $\mathbf{r}^2 \phi = \mathbf{r} \cdot \mathbf{B}$
- Correct B at faces: $B = B - r f$
- Correct the fluxes $F^{n+1/2}_{i+1/2,j}$ with projected values of B
- Update conservative variables using the fluxes
 - *The non-conservative source term $S(U)$ a $\mathbf{r} \cdot \mathbf{B}$ has been algebraically removed*
- On uniform Cartesian grids, projection provides the smallest correction to remove the divergence of B . (Toth, JCP 2000)
- Does the nature of the equations change?
 - *Hyperbolicity implies finite signal speed*
 - *Do corrections to B via $\mathbf{r}^2 f = \mathbf{r} \cdot \mathbf{B}$ violate hyperbolicity?*
- Conservation implies that single isolated monopoles cannot occur. Numerical evidence suggests these occur in pairs which are spatially close.
 - *Corrections to B behave as a $1/r^2$ in 2D and $1/r^3$ in 3D*



• Projection does not alter the order of accuracy of the upwinding scheme and is consistent

Unsplit + Projection AMR Implementation

- Implemented the Unsplit method using Chombo
- Solenoidal B is achieved via projection, solving the elliptic equation $\mathbf{r}^2 \phi = \mathbf{r} \cdot \mathbf{B}$
 - Solved using Multigrid on each level (union of rectangular meshes)
 - Coarser level provides Dirichlet boundary condition for f
 - Requires $\mathcal{O}(h^3)$ interpolation of coarser mesh f on boundary of fine level
 - a “bottom smoother” (conjugate gradient solver) is invoked when mesh cannot be coarsened
- Multigrid convergence is sensitive to block size
- Flux corrections at coarse-fine boundaries to maintain conservation
 - A consequence of this step: $\mathbf{r} \cdot \mathbf{B} = 0$ is violated on coarse meshes in cells adjacent to fine meshes.

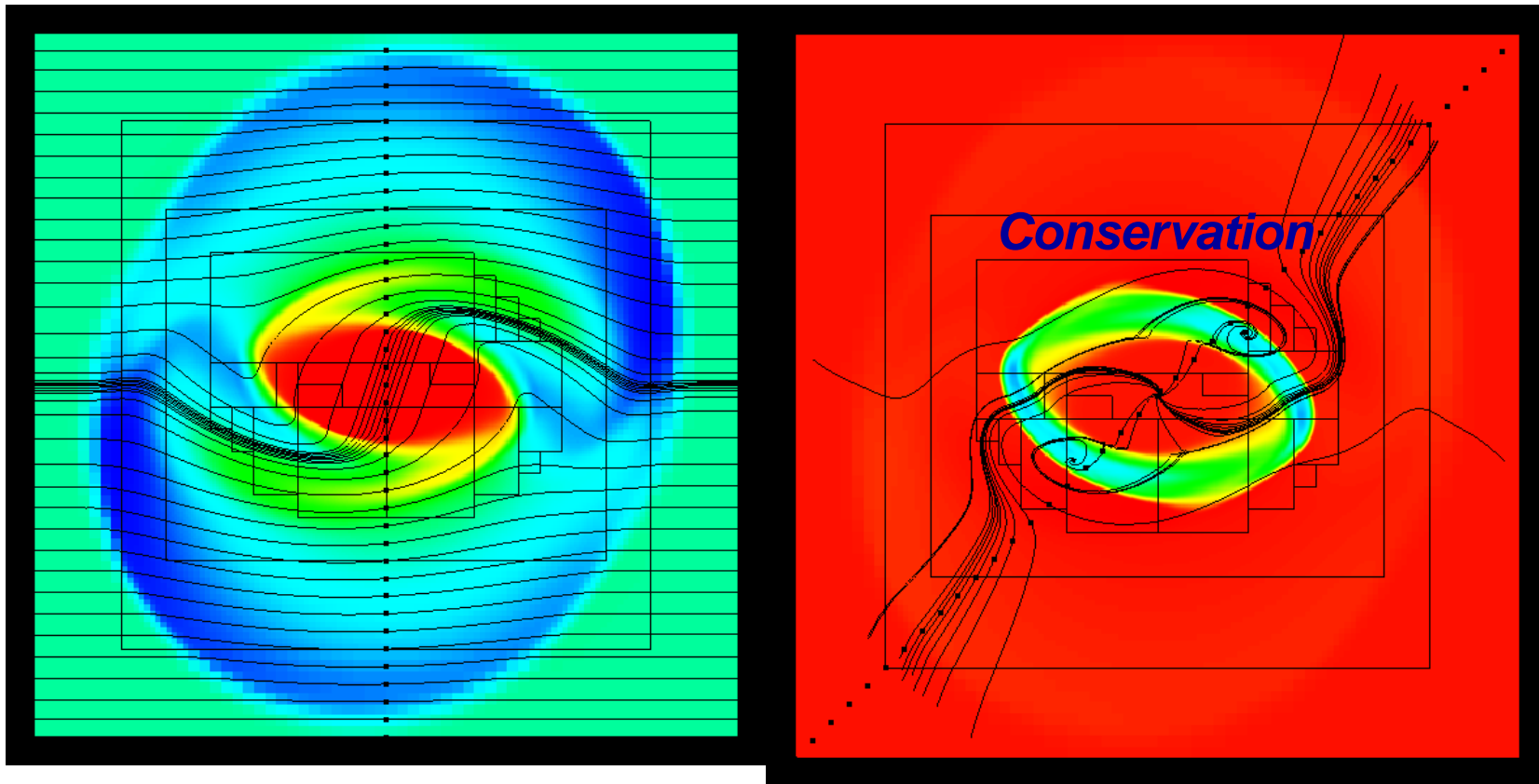


Implicit treatment of parabolic flux terms

- Implicit treatment requires the solution of elliptic equations (Helmholtz equation)
 - *Completed implicit treatment of viscous, heat conduction and resistive terms*
 - *Viscous and conduction terms require non-constant coefficient Helmholtz solvers - Completed*
 - *Favored approach: Implicit Runge Kutta, TGA Approach (Twizell, Gumel, Arigu, Advances in Comp. Math. 6(3):333-352, 1996)*
 - *Due to C++ abstractions, other solvers (Backward Euler, Crank-Nicholson) can also be used instead of TGA – choice can be made by the user.*
 - *$r\phi u$ is ignored in the shear stress tensor. If $r\phi u$ is included, the resulting elliptic equations are coupled -such solvers are under development*
- Quadratic interpolation ($O(h^3)$) at coarse-fine boundaries
 - *Corner terms required and obtained by linear interpolation*
- Flux-refluxing step requires implicit solution on all levels synchronized at the current time step.
 - *Backward Euler used for this step*



Weak rotor – Resistive MHD



Pressure with B field lines

r with velocity streamlines

Pellet Injection: Objective and Motivation

- Objectives
 - *Identify the mechanisms for mass distribution during pellet injection in tokamaks*
 - *Quantify the differences between “inside launch” and “outside launch”*
- Motivation
 - *Fusion power depends upon efficient fueling*
 - *Gas puffing is limited in its ability to achieve core fueling*
 - *Injection of frozen hydrogen pellets is a viable method of fueling a tokamak (Bell et al., Nuclear fusion, 2000)*
 - *Pellet injection provides much deeper fueling*
 - *Pellet-plasma interactions:*
 - *Ablation: Considered well-understood*
 - *Mass deposition: Large scale MHD driven but poorly understood*



Background - Experimental

- Early pellet experiments showed improvement in energy confinement with pellet fueled plasmas (Greenwald, PRL, 1984)
- Pellet injection of frozen hydrogen is a viable method to fuel tokamaks (Bell et al., Nuclear Fusion 1992 – this TFTR experiment also exceeded empirical Greenwald density limit)
- Inside (HFS) vs. outside (LFS) launch
 - *HFS is more effective in fueling the center of the plasma (Lang et al. PRL 1997, Baylor et al. Phys. Plasmas 2000)*
 - *Example: DIII-D fueling efficiency is 95% (HFS), 55% (LFS)*
- Pellets trigger formation of internal transport barrier with central heating
- Edge localized modes are triggered in H-mode by strong perturbations from pellets



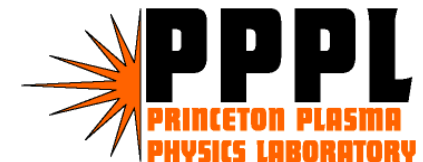
Background – Simulation/Theory

- Earliest ablation model by Parks (Phys. Fluids 1978)
 - *Accurate expression for pellet ablation once pellet is in contact with the high temperature plasma*
- Detailed multi-phase calculations in 2D of pellet ablation (MacAulay, PhD thesis, Princeton Univ 1993, Nuclear Fusion 1994)
 - *Agreement with Parks model of plasma ablation within a factor of 2*
- 3D Simulations by Park and Strauss (Phys. Plasmas, 1998)
 - *Solve an initial value problem . Initial condition consists of a prescribed MHD equilibrium and a large density “blob” to mimic a fully ablated pellet cloud with zero flux averaged pressure perturbation*
 - *Pellet cloud to device dimension was relatively large due to resolution restrictions*
 - *No motion of pellet modeled*
 - *Mass distribution along field lines*
 - *Scaling law for mass distribution established*
 - *Verified that MHD effects cause localized density perturbation to displace towards LFS.*



Approach/ Model

- Detailed 3D AMR simulations of pellet injection – pellet treated as moving density source
 - *Ratio of pellet size to device size is $\sim O(10^{-3})$*
- Phased approach
 - *Simple Cartesian geometry AMR simulation to understand the basic physics of mass redistribution with varying degrees of complexity*
 - *Ideal MHD with density and energy source terms*
 - *Resistive MHD with density source and anisotropic heat conduction*
 - *Force terms to mimic toroidal geometry*
- Physical assumptions for first phase of AMR simulations
 - *Pellet ablates with an analytic ablation model*
 - *Instantaneous heating of ablated mass by electrons to corresponding flux surface temperature*
 - *No drag coupling between pellet and ambient plasma*
 - *Single fluid/single phase*
- Mathematical model is Ideal MHD with source terms in density and energy equations



Mathematical Model I

- Mass conservation $\frac{\partial n}{\partial t} + \nabla \cdot (n \vec{V}) = \frac{dN}{dt} \delta(\vec{X} - \vec{X}_p(t))$

Mass source active on pellet surface

- Momentum conservation $nM_i \left(\frac{\partial \vec{V}}{\partial t} + \vec{V} \cdot \nabla \vec{V} \right) = \vec{J} \times \vec{B} - \nabla p - \vec{T}_1$

- Maxwell equations $\frac{\partial \vec{B}}{\partial t} = -\nabla \times \vec{E}$

Maxwell equations

$$\vec{E} + \vec{V} \times \vec{B} = \eta \vec{J} + \vec{T}_3$$

Toroidal source terms zero in Cartesian geometry

$$\mu_0 \vec{J} = \nabla \times \vec{B}$$

Energy conservation

$$\frac{\partial p}{\partial t} + \vec{V} \cdot \nabla p = -\frac{5}{3} p \nabla \cdot \vec{V} + \frac{2}{3} [\eta J^2 + \nabla \cdot \vec{q}] + \vec{T}_2$$



Mathematical Model II

- Mass source is given using the ablation model by Kuteev (Nuclear Fusion 1995)

$$\frac{dN}{dt} = -4\pi r_p^2 \frac{dr_p}{dt} 2n_m = 1.12 \times 10^{16} n_e^{0.333} T_e^{1.64} r_p^{1.33} M_i^{-0.333}$$

- Pellet shape is spherical for all t
- Above equation uses cgs units
- Delta function in source term approximated as a “top-hat” function of width ten times the pellet radius (motivated by Parks et al. Phys. Plasmas 2000)
- For numerical computations, equations re-written in strong conservation form
- Energy equation source term: $dN/dt \times 3T/2$ where T is the temperature of the flux surface at the pellet center to model heating by electrons on the flux surface

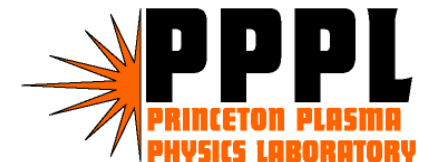
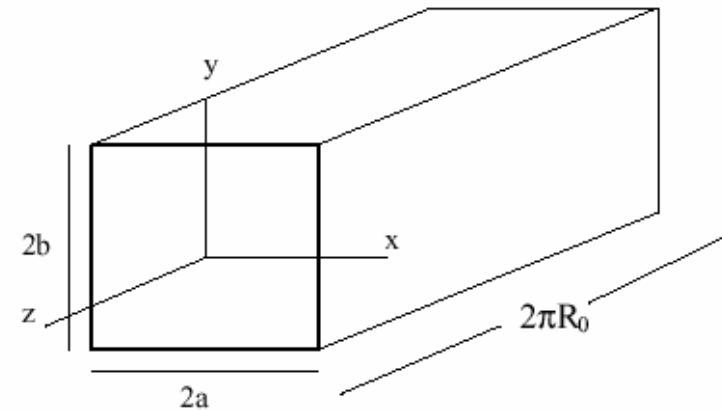


AMR Simulation Parameters

- Toroidal Magnetic Field
 $B_T=0.2$ T
- Device size $a=0.2$ m
- Initial Pellet size $r_p=0.1$ cm
- Pellet velocity $v_p=3000$ m/s
- Plasma $\beta=0.1$
- Average plasma Temperature $T=662$ eV
- Initial average density $n=1.5 \times 10^{19}/\text{m}^3$
- Boundary conditions: $\mathbf{B}_n \cdot \mathbf{n}=0$, $u \cdot \mathbf{n}=0$ on sides
Periodic in z-direction
- Initial condition: Ideal MHD equilibrium
 $\psi = \psi_0 \sin k_x x \cos k_y y$

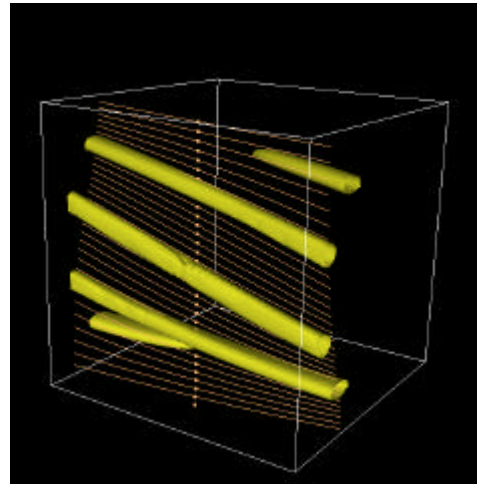
$$\rho = \rho_0 + \rho_1 \psi^2$$

$$\mathbf{B} = \nabla \psi \times \mathbf{r} + B_T \mathbf{k}$$

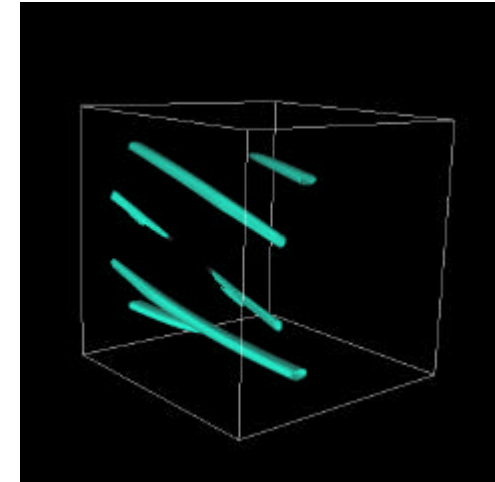


Results from AMR Simulations –Early time

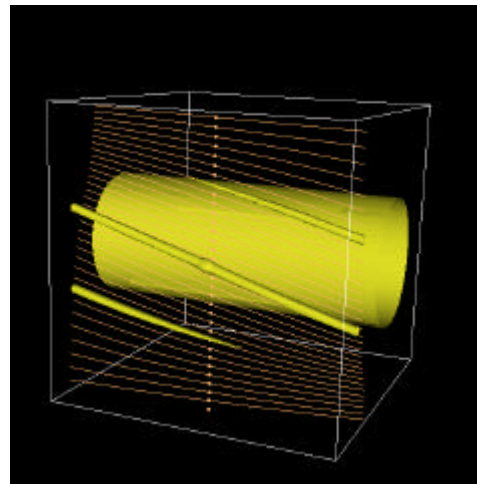
- Observations
 - *Even at early time, mass is rapidly distributed along field lines, and shows the appearance of striations (consistent with experimental observations)*



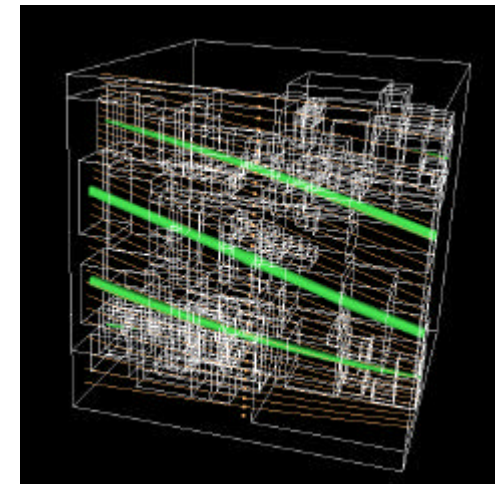
$t=0.66. r$



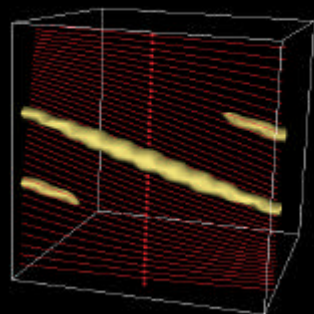
Mach No. (Peak 0.3)



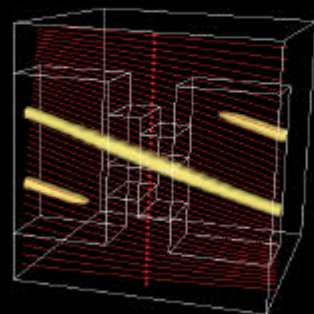
Pressure



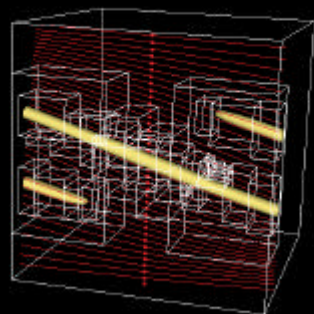
Results from AMR Simulations –Early time



Level 0

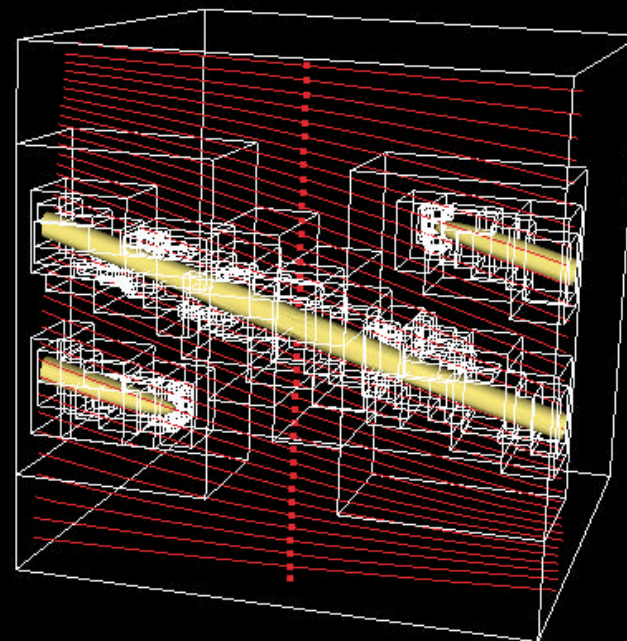


Level 0-1



Level 0-2

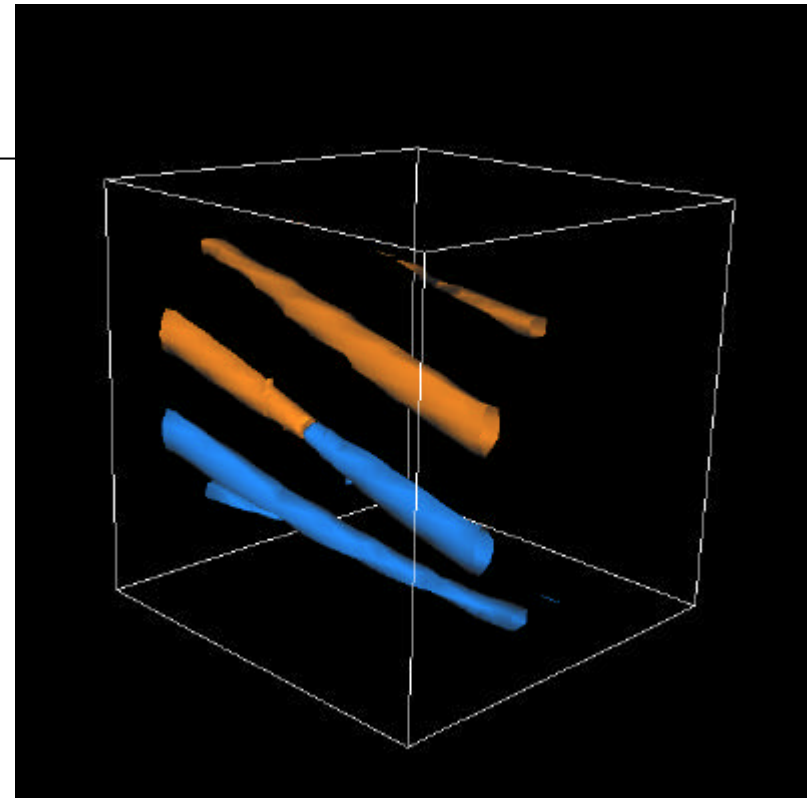
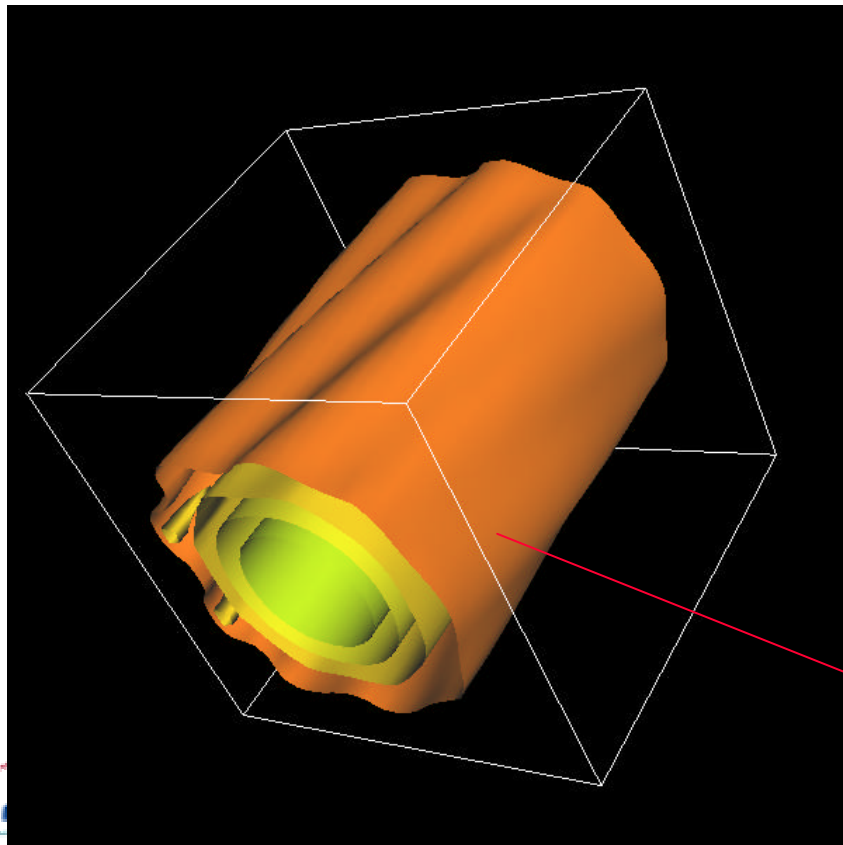
Density isosurfaces at $t=0.45$. Boxes indicate meshes at various AMR levels. Equivalent uniform mesh resolution: 512^3



Level 0-3

Results from AMR Simulations

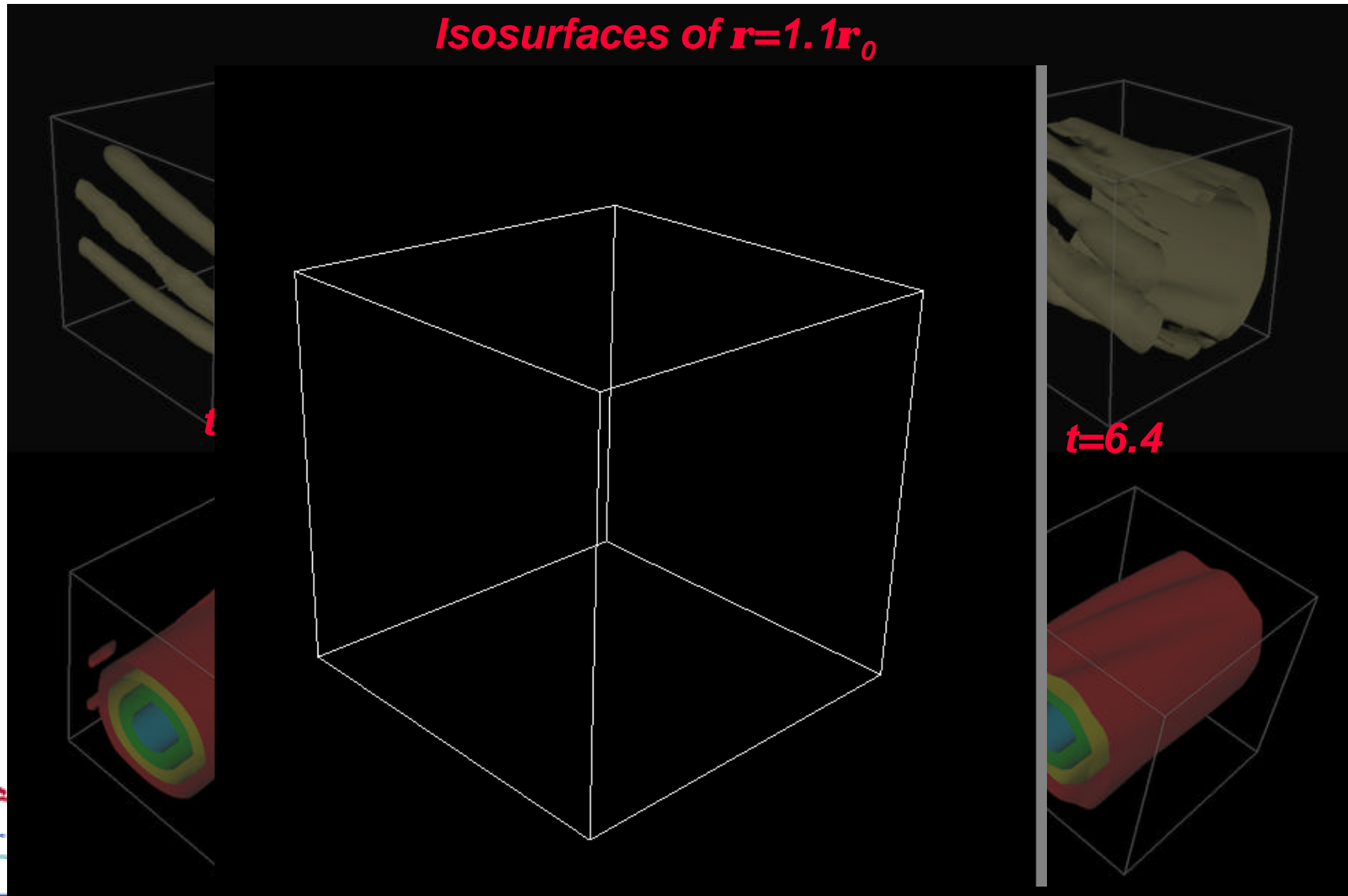
Parallel velocity isosurfaces at $t=3.86$



*$t=3.86$ Isosurfaces of plasma b
 $b_{max}=0.51$ at the pellet surface*

Results from AMR Simulations

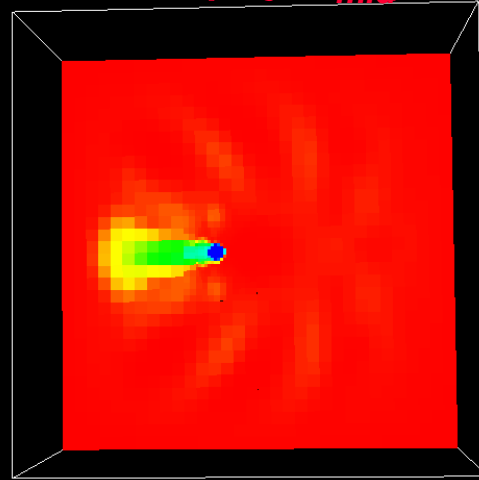
Isosurfaces of $r=1.1r_0$



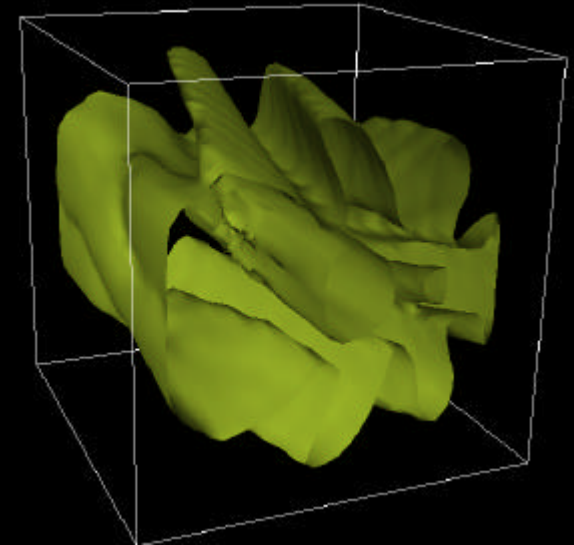
Results from AMR Simulations

$t \sim 25$

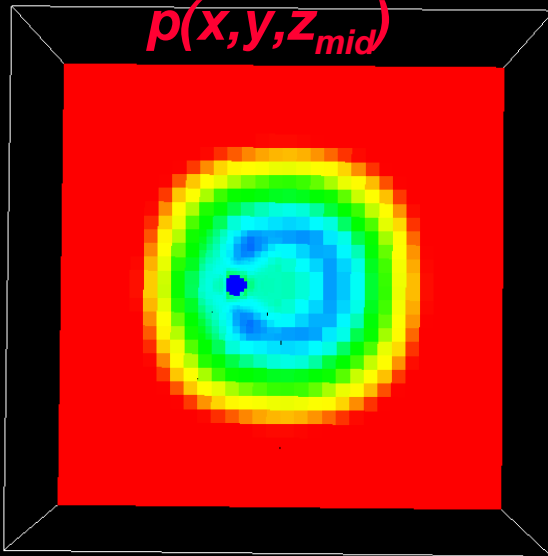
$r(x, y, z_{mid})$



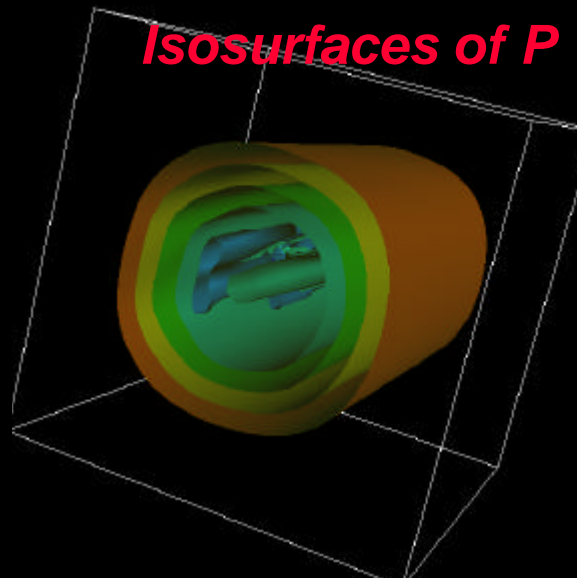
$r = 1.1r_0$



$p(x, y, z_{mid})$



Isosurfaces of P



Conclusion and Future Work

- First 3D AMR simulations of pellet injection in Cartesian geometry
 - *Includes model for pellet ablation and prescribed motion of pellet*
 - *Ablated mass is distributed along field lines*
 - *This preliminary study indicates that AMR is a viable approach to efficiently resolve the relatively small pellet*
- A conservative solenoidal B AMR MHD code was developed in 3D using the Chombo framework
 - *Unsplit upwinding method for hyperbolic fluxes*
 - *$\nabla \cdot B=0$ achieved via projection*
- Future Work
 - *Toroidal forcing terms to mimic tokamak geometry*
 - *Investigate LFS and HFS pellet-launches*
 - *Better treatment of energy equation*
 - *Inclusion of anisotropic heat conduction*
 - *Realistic device parameters*

